

UCLA

UCLA Previously Published Works

Title

Preliminary observations in support of the development of an ergodic site response model in California conditioned on Vs30 and HVSR Parameters

Permalink

<https://escholarship.org/uc/item/3527w1wb>

Authors

Ornelas, Francisco-Javier G

Buckreis, Tristan

Nweke, Chukwuebuka C

et al.

Publication Date

2024-05-07

Peer reviewed

Preliminary observations in support of the development of an ergodic site response model in California conditioned on V_{S30} and HVSR Parameters

Francisco-Javier G. Ornelas ⁱ⁾, Tristan E. Buckreis ⁱⁱ⁾, Chukwuebuka C. Nweke ⁱⁱⁱ⁾, Pengfei Wang ^{iv)}, Christopher de la Torre, ^{v)}, Scott J. Brandenburg ^{vi)} and Jonathan P. Stewart ^{vii)}

- i) Graduate Student Researcher, Department of Civil Engineering, UCLA, 580, Portola Plaza, Los Angeles, CA 90095, USA.
- ii) Post Doctoral Researcher, Department of Civil Engineering, UCLA, 580, Portola Plaza, Los Angeles, CA 90095, USA.
- iii) Professor, Department of Civil Engineering, USC, 3620, Vermont Ave., Los Angeles, CA 90089, USA.
- iv) Professor, Department of Civil Engineering, Old Dominion University, 5115, Hampton Blvd, Norfolk, VA 23529, USA.
- v) Post Doctoral Researcher, Department of Civil Engineering, UC, 20 Kirkwood Ave., Christchurch, 8041, NZ.
- vi) Professor, Department of Civil Engineering, UCLA, 580, Portola Plaza, Los Angeles, CA 90095, USA.
- vii) Professor, Department of Civil Engineering, UCLA, 580, Portola Plaza, Los Angeles, CA 90095, USA.

ABSTRACT

Traditional ergodic models are derived based on time-averaged shear-wave velocity in the upper 30 m of the site. These models are not able to account for site resonances, the presence and frequency of which can be established from microtremor HVSR surveys. Not all California sites exhibit such resonances, but knowledge that peaks are or are not present affects site response over a wide range of frequencies, with the former producing a response spectral peak near the HVSR peak. Research is underway to develop a model using microtremor HVSR data, which will be novel relative to previous models that are based on earthquake HVSR data. Our model is being formulated as modification to a global V_{S30} and $z_{1.0}$ relationship. This paper explains the model development approach and findings of a systematic assessment of how HVSR curves relate to features of site-specific (or non-ergodic) response, which is informing model development.

Keywords: Microtremors, HVSR, Site Response, Ground Motion Model

1 INTRODUCTION

Ground motion models (GMMs) used in California include components for source, path and site effects and are derived from global databases (e.g., Next Generation Attenuation [NGA] West2 Project: Bozorgnia et. al. 2014). These GMMs are referred to as ergodic (Anderson and Brune 1999) because they are derived from global data and in application are assumed to apply to a specific site in a specific region. The site components of these models are conditioned on time-averaged shear wave velocity to 30 m depth (V_{S30}) and depth to the 1.0 or 2.5 km/s shear-wave velocity (V_S) isosurfaces (denoted $z_{1.0}$ and $z_{2.5}$, respectively), and may over or under predict the true site response of a site in a particular region. In particular, these models also do not capture site resonances which can occur at sites with significant impedance contrasts.

Microtremor horizontal-to-vertical spectral ratios (mHVSR) provide information that can identify such resonances. mHVSR spectra are computed by taking the ratios of the Fourier amplitude spectra (FAS) of horizontal-to-vertical components of microtremor recordings (e.g., Nakamura 1989). Previous research that

has used HVSR to improve site amplification models have generally used the peak frequency (f_p) from mHVSR in combination with V_{S30} (Harmon et. al. 2019; Hassani and Atkinson, 2018a, 2018b; Kwak et. al. 2017; Wang et. al. 2022; Buckreis et. al. 2023a). Limitations of previous methods are that they are applied to small areas or were derived from earthquake HVSR, hence they are not applicable for broad regions like California.

In this paper, we describe the approach we are using and provide examples of how mHVSR is and is not related to site response. The models are not yet available. Our ultimate objective is to provide models that can be used with mHVSR data to reduce bias and uncertainty in estimates of linear site amplification at California sites.

2 HVSR

We use mHVSR data from the Shear Wave Velocity Profile DataBase (VSPDB; Kwak et. al. 2021). There are two general data sources: (1) vibrations recorded by permanently-installed seismometers, (2) vibrations recorded during surveys in which a 3-component seismometer is temporarily deployed for a period of time (typically ~1-2 hr.). Sources of the vibrations recorded

in these surveys include shear and surface waves induced by sources such as anthropogenic, wind, and ocean waves. The data is processed using procedures outlined in Wang et. al. (2023), which are more applicable to California than previous procedures (e.g., SESAME 2004).

We queried an expanded ground motion database, relative to NGA-West2, (Buckreis et al. 2023b) to identify stations where mHVSr surveys had been done. The total number of California stations with earthquake ground motion data in the database is 3322. Of those, 471 sites were found to contain mHVSr surveys within a 150-meter radius. We then screened the sites to remove those with < 4 recordings of $\mathbf{M} > 4$ earthquakes (this was done so that site terms derived from earthquake data, used to compare against mHVSr spectra, are reasonably stable). Following this screen, 371 sites have mHVSr curves and enough earthquake recordings to derive site terms using non-ergodic procedures (Stewart et al. 2017).

For each of the 371 sites, we identify whether an mHVSr peak is present using the algorithm presented by Wang et. al. (2023). The algorithm uses a regression tree approach to represent the mHVSr curve as a step-wise function, which stabilizes (i.e., smooths) the amplitudes. A peak is identified when the stabilized amplitude of a peak relative to neighboring stabilized amplitudes is sufficiently high (generally more than a factor of two) and the variability in the amplitudes is sufficiently small. The outcome is 220 (59%) of sites have peaks. For sites with peaks, a Gaussian function is fit to the peak (Ghofrani and Atkinson 2014):

$$F_{H/V,i} = c_{0,i} + c_{1,i} \exp \left[-\frac{1}{2} \left(\frac{\ln(f/f_{p,i})}{2w_{p,i}} \right)^2 \right] \quad (1)$$

where $f_{p,i}$ is the fitted peak frequency for the i^{th} HVSr peak, c_1 is the peak amplitude, w_p is the peak width, c_0 is a frequency-independent constant, and f is frequency in Hz. The absolute amplitude of the peak is computed as, $a_p = c_0 + c_1$. Figure 1 shows mHVSr for two example sites; station 62 has a peak that is fit using Eq. (1) and station 199 lacks a peak. The parametrization of peaks will aid in model development, as shown subsequently.

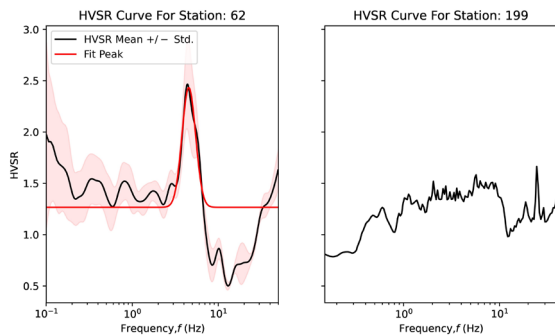


Fig. 1. mHVSr curves for two example sites with and without peaks. Red line represents the Gaussian pulse fit (Eq. 1).

3 SITE RESPONSE ESTIMATES FROM DATA

For each of the 371 sites identified as described in Section 2, we applied non-ergodic site response methods to estimate the site-specific linear amplification. This provides the site response estimates that are compared to mHVSr (next section). This analysis begins by computing total residuals (δ_{ij}) for site j in event i as the difference between the observed intensity measure (Y_{ij}) and the median predictions of a GMM (μ_{ij}):

$$\delta_{ij} = \ln(Y_{ij}) - \mu_{ij}(\mathbf{M}, R_{jb,ij}, V_{S30,j}, z_{1.0,j}) \quad (2)$$

The total residuals were then partitioned into fixed and random effects using mixed effects analyses (Abrahamson and Youngs 1992, Gelman and Hill 2006; Sahakian et. al. 2018) as expressed below:

$$\delta_{ij} = c_k + \eta_{E,i} + \eta_{S,j} + \varepsilon_{ij} \quad (3)$$

where c_k represents the model bias for GMM k , η_E and η_S are random effects that quantify event- and site-specific biases, respectively, and ε is the remaining portion of the within-event residual after systematic site effects are removed. The total linear site response relative to a reference condition of $V_{S30}=760$ m/s is given as (Stewart et al. 2017),

$$(f_1)_j = F_{lin}^{erg} + \eta_{S,j} \quad (4)$$

where f_1 is the total site response for linear conditions, F_{lin}^{erg} is the ergodic model prediction of site response (using the same GMM as applied in the residuals calculation), and η_S is the site term, as before. Epistemic uncertainty of the total site response can be taken as the standard error of the site term, and hence inversely scales with the square root of the number of ground motion recordings at site j .

4 RELATING SITE RESPONSE TO MHVSr

Figure 2 shows example results for three sites with site response peaks. The figures are formatted to show on a single figure the residual site response after first- and second-order site effects have been modelled by V_{S30} and $z_{1.0}$, respectively and the frequency-dependent mHVSr. The frequencies shown on the abscissa have different meanings, with site response using oscillator frequency and mHVSr using frequency as used with FAS. The mHVSr mean curves and \pm one standard deviation from the data are shown and, if a peak was identified, the fit per Eq. (1) is shown. The site response is shown as a mean curve (Eq. 4) with a shaded band that indicates \pm one standard error.

Figure 2(a) has a two-sided peak in the site response at 1.2 Hz. The peak aligns with an mHVSr peak at approximately the same frequency, although the site response peak is much smaller in amplitude. It is typical for the site response peaks to be less prominent as shown by this example. Figures 2(b) and 2(c) show one-sided

peaks. Figure 2(b) is considered a left-sided peak (site response is low to the left and either peaks or becomes flat at the peak frequency and to the right) whereas Figure 2(c) is a right-sided peak. Sites with left-sided peaks (Fig. 2(b)) often have mHVSr peaks at the transition frequency; these cases typically involve high frequency peaks (roughly 5Hz or greater). On the other hand, right-sided peaks (Fig. 2(c)) also often have mHVSr peaks at the transition frequencies, which are typically fairly low (roughly 0.5 Hz or less).

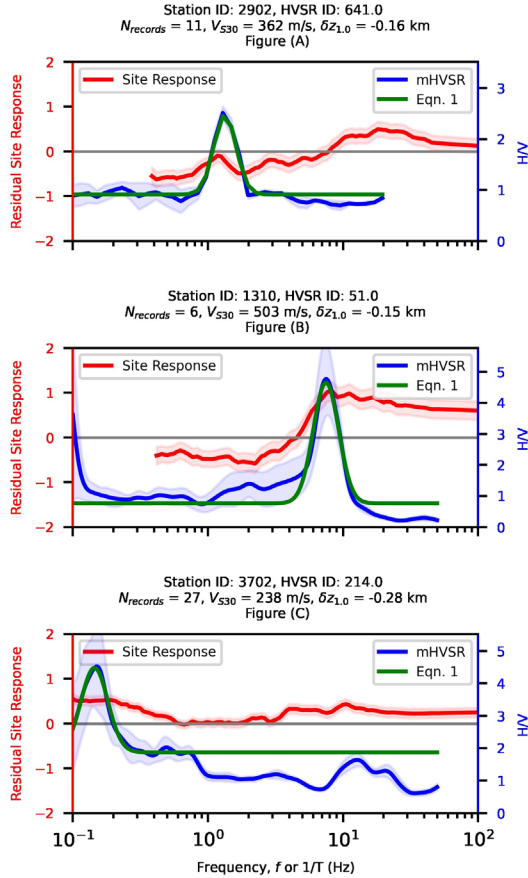


Fig. 2. Plots for example sites of frequency-dependent site response (each example has a peak) and mHVSr, with peak fits where applicable. Fig. 2(a) represents station 2902 which is experiencing a two-sided peak feature. Fig. 2(b) represents station 1310 which is experiencing a one-sided peak condition. Fig. 2(c) represents station 3702 which is experiencing a one-sided peak condition.

The examples of “ramped” site response in Figures 2(b) and 2(c) are relatively common. This occurs because the ergodic model reasonably captures the site response at either short- or long-periods (below the ramp) but over-predicts outside of that range (above the ramp). Anecdotally, it appears that mHVSr may hold some promise for identifying the transition frequencies for this behavior. Whether it can distinguish this ramped behavior from true peak behavior (Fig. 2(a)) remains to be evaluated.

Some sites lack site response peaks. Figures 3(a) and 3(b) show sites without site response peaks in which mHVSr has a peak (Fig. 3(a)) and does not have a peak (Fig. 3b). The case in Figure 3(a) can be considered a false positive (mHVSr predicts a peak where none is present) whereas Figure 3(b) shows a true negative (mHVSr predicts no peak where none is indeed present).

We anticipate the site response peaks will ultimately be modelled using Gaussian or Mexican Hat pulse functions. Logistic functions could potentially be used to model ramped responses.

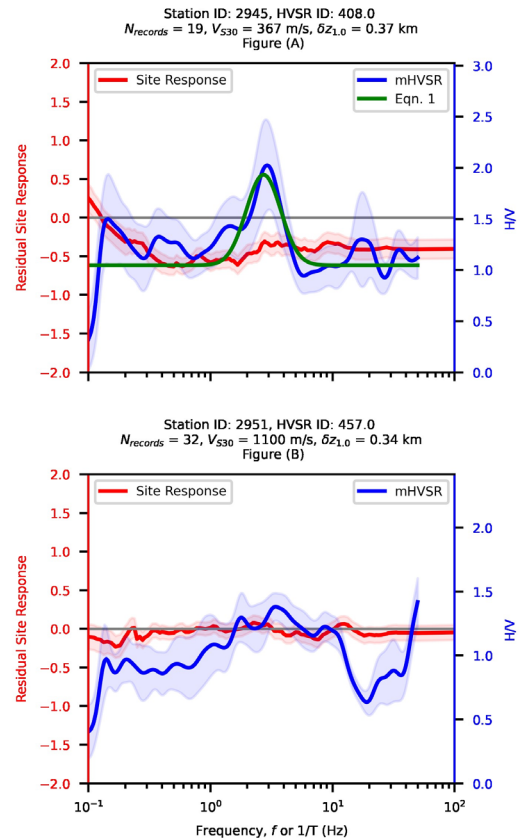


Fig. 3. Plots for example sites of frequency-dependent site response and mHVSr for example sites without site response peaks. Fig. 3(a) represents station 2945 which experiencing a peak in mHVSr, but not in site response. Fig. 3(b) represents station 2951 which is experiencing no peak in mHVSr and site response.

5 MODEL DEVELOPMENT APPROACH

We will apply a model development approach that was originally formulated to produce a combined V_{s30} and HVSR model for site response in the Delta region of California by Buckreis et al. (2023a). The steps in this procedure are as follows:

1. Identification of site parameters from mHVSr: Evaluate whether mHVSr spectra contain peaks and the properties of those peaks, as described in Section 2.

2. Derive non-ergodic site responses: Utilize ground motion data to derive site terms and site response as provided in Eq. (4) and described in Section 3.
3. Parametrize site response peaks or ramps: Fit appropriate peak or ramp functions to the data and evaluate for each site the parameters describing those functions. For example, whether a peak or a ramp, one parameter would be the frequency where the central part of the feature occurs.
4. Formulate model for site response peak probability: A model is needed for the probability that a site response peak of the types shown in Figure 2 is present, conditioned on mHVSr attributes. We anticipate that sites with large-amplitude, narrow peaks that occur at frequencies < 10 Hz are likely to have site response peaks.
5. Formulate site amplification model: We envision a site amplification model that would be additive (in natural log units) with the amplification from a model with V_{S30} - and $z_{1.0}$ -scaling,

$$F_{Sm} = F_S + F_{HV} \quad (5)$$

Where F_S is the V_{S30} - and $z_{1.0}$ -scaling model and F_{HV} is the model conditioned on HVSR parameters. For sites with mHVSr peaks, the F_{HV} model will be formulated so that the flat zones to the left and right of the peaks can have different amplitudes, to capture the different behaviors shown in Figure 2. The parameters describing the F_{HV} function will be related to mHVSr attributes. For sites without mHVSr peaks, F_{HV} will be a constant,

$$F_{HV} = \bar{c} \quad (6)$$

where the constant will be related to the mHVSr amplitude. The final site response model will include a prediction for cases where a peak is present (scaled by the peak probability) and a prediction for cases where the peak is absent (scaled by one minus the peak probability).

Steps 4 and 5 are under development for the state of California, but models for these effects in the Delta region have been presented by Buckreis et al. (2023a). The resulting models would apply across California and would be most reliable in areas with ample ground motion recording stations.

6 SUMMARY

We have presented the approach we are applying to develop a model to couple HVSR parameters with V_{S30} and $z_{1.0}$ for site response prediction. The motivation for using both parameters is that V_{S30} is known to provide a generally effective estimate of site response over a wide period range, whereas HVSR parameters have predictive power near identified peaks. The model will be

applicable to California as a whole. The results from example sites showing the relationship between site response and HVSR are encouraging regarding the potential correlations. The model produced by this effort has the potential to significantly impact site response estimation in the United States, where HVSR is not typically considered in practice.

ACKNOWLEDGEMENTS

The research presented here was supported by a research gift from Pacific Gas and Electric Company. This support is gratefully acknowledged.

REFERENCES

- 1). Abrahamson, N.A. and Youngs, R.R. (1992): A stable algorithm for regression analyses using the random effects model. *Bulletin of the Seismological Society of America* 82, 505–510.
- 2). Anderson, J.G., and Brune J.N. (1999): Probabilistic seismic hazard assessment without the ergodic assumption, *Seismol. Res. Lett.* 70, 19–28.
- 3). Bozorgnia, Y., Abrahamson, N.A., Al Atik, L., Ancheta, T.D., Atkinson, G.M., Baker, J.W., Baltay, A., Boore, D.M., Campbell, K.W., Chiou, B.S.-J., Darragh, R., Day, S., Donahue, J., Graves, R.W., Gregor, N., Hanks, T., Idriss, I.M., Kamai, R., Kishida, T., Kottke, A., Mahin, S.A., Rezaeian, S., Rowshandel, B., Seyhan, E., Shahi, S., Shantz, T., Silva, W., Spudich, P., Stewart, J.P., Watson-Lamprey, J., Wooddell, K., and Youngs, R. (2014): NGA-West2 research project. *Earthquake Spectra* 30(3), 973-987.
- 4). Buckreis, T.E., Stewart, J.P., Brandenburg, S.J., and Wang, P. (2023a): Small-strain site response of soft soils in the Sacramento-San Joaquin Delta region of California conditioned on V_{S30} and mHVSr, *Earthquake Spectra*, DOI: 10.1177/87552930231217165/
- 5). Buckreis, T.E., Nweke, C.C., Wang, P., Brandenburg, S.J., Mazzoni, S., and Stewart, J.P. (2023b): Relational database for California strong ground motions, *Geo-Congress 2023: Geotechnical Data Analysis and Computation*, Los Angeles, CA, March 2023, *Geotechnical Special Publication* 342, 461-470.
- 6). Gelman, A. and Hill, J. (2006): *Data analysis using regression and multilevel/hierarchical models*, 1st edition, CRC press.
- 7). Harmon, J., Hashash, Y.M.A., Stewart, J.P., Rathje, E.M., Campbell, K.W., Silva, W.J. and Ilhan, O. (2019): Site amplification functions for central and eastern North America—Part II: Modular simulation based models. *Earthquake Spectra* 35(2), 815–847.
- 8). Hassani, B. and Atkinson, G.M. (2018a): Application of site-effects model based on peak frequency and average shear-wave velocity to California. *Bulletin of the Seismological Society of America* 108(1), 351-357.
- 9). Hassani, B. and Atkinson, G.M. (2018b): Site-effects model for central and eastern North America based on peak frequency and average shear-wave velocity. *Bulletin of the Seismological Society of America* 108, 338-350.
- 10). Kwak, D.Y., Stewart, J.P., Mandokhail, S.J., and Park, D. (2017): Supplementing V_{S30} with H/V spectral ratios

- for predicting site effects. *Bulletin of the Seismological Society of America* 107(5), 2028-2042.
- 11). Kwak, D.Y., Ahdi, S.K., Wang, P., Zimmaro, P., Brandenberg, S.J. and Stewart, J.P. (2021): Web portal for shear wave velocity and HVSR databases in support of site response research and applications. UCLA Geotechnical Engineering Group. DOI:10.21222/C27H0V
 - 12). Nakamura, Y. (1989): A method for dynamic characteristics estimation of subsurface using microtremor on the ground surface. *Quarterly Report of Railway Technical Research* 30(1), 25–33
 - 13). Site EffectS assessment using AMbient Excitations (SESAME) (2004): Guidelines for the implementation of the H/V spectral ratio technique on ambient vibrations—Measurements, processing and interpretation, European Commission, Project No. EVG1-CT2000-00026, available at http://sesame.geopsy.org/Papers/HV_User_Guidelines.pdf
 - 14). Wang, P., Tsai, Y.T., Stewart, J.P., Mikami, A. and Brandenberg, S.J. (2022a): Region-specific linear site amplification model for peaty organic soil sites in Hokkaido, Japan. *Earthquake Spectra* 38(3), 2207-2234.
 - 15). Wang, P., Zimmaro, P., Ahdi, S.K., Yong, A. and Stewart, J.P. (2023): Identification protocols for horizontal-to-vertical spectral ratio peaks. *Bulletin of the Seismological Society of America* 113(2), 782 – 803.